ARCHIVES of FOUNDRY ENGINEERING

Published quarterly as the organ of the Foundry Commission of the Polish Academy of Sciences

ISSN (1897-3310)
Volume 13
Special Issue
1/2013
21–25

5/1

Characteristics of the Geometric Structure of Metal Foams

K. Gawdzińska *, J. Grabian, W. Przetakiewicz

Maritime University of Szczecin, 70-500 Szczecin, Wały Chrobrego 1–2, Poland
* Corresponding author. E-mail address: k.gawdzinska@am.szczecin.pl

Received 28.01.2013; accepted in revised form 08.05.2013

Abstract

A description of material should include its characteristic properties. Metal foams, however, lack such descriptions. This author proposes a description of geometric structure of these materials and divides characteristics of the structure geometry into four groups: porosity, shape and size of pores, actual to maximum porosity ratio, specific surface area of bubbles and the homogeneity of the foam structure, divided, in turn, into the homogeneity of pore size, shape and distribution. This study is an open proposition of a description of metal foam geometric structure.

Keywords: Metal composite foams, Geometric properties of a structure

1. Introduction

The geometric spatial structure of foams can be examined by means of tools, known in stereology and statistics, facilitating the description of this geometry. Apart from foam geometry description, that is the description of material discontinuities (pores) distributed in an orderly or disorderly manner, methods of spatial (3D) imaging – computer tomography – can be employed. Image analysis, covering both macro- or microscopic images (mostly using an optical or scanning electron microscope), is used for quantitative description of material structure. Methods of computer-based image analysis are also useful for determining morphological properties of a material. These automatic methods allow to significantly minimize the duration of measurements, compared to traditional methods. Computer-based image analysis enables a full description of the examined material structure, by using various geometric parameters, often unavailable in previously used methods. The application of stereological and statistical tools allows to make an objective evaluation of structure properties comprising a very large number of images. Thus, the evaluation results can be transferred onto macro-structural properties of the examined material [1–3].

Metal foam can be characterized by these basic properties:

- porosity,
- shape and size of pores,
- ratio of actual to maximum porosity,
- specific surface area of bubbles,
- foam homogeneity:
  – homogeneity of pore size and shape,
  – homogeneity of pore distribution.

Presented below is the author's description geometric structure of metal foams.

2. Methods of describing the geometric structure of foams

Porosity

The value of foam porosity can be calculated from this relationship [4]:

$$P = 1 - \frac{\rho_p}{\rho_m} \qquad (1)$$

where:

ρ_p – apparent density of metal foam sample,
ρ_m – density of metal making up the foam.

Porosity can also be determined by an image analysis of foam sample cross-section using the principles of stereometry. Bubbles in the metal are spherical in shape when they are being formed. If they remained spherical till the end, the foam porosity, if we assume that metal walls around each bubble are infinitely thin, could not exceed a value of 74.4% (1). To obtain higher degree of porosity requires that bubbles should become deformed when getting in contact with other bubbles, as depicted in Fig. 1.

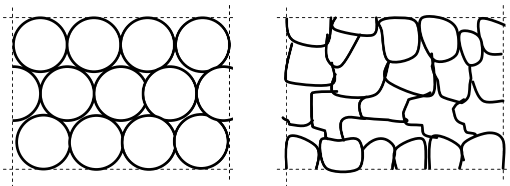

Fig. 1. The relationship between porosity and pore shape [5]

The fact that real foam consists of deformed pores is displayed in Fig. 2, a view of aluminum foam cross-section, well described in A.M. Kraynik's considerations [6].

Fig. 2. Shapes of aluminum foam pores

Pore shape and size

In practice, the shapes and sizes of pores can be described geometrically as shown in Fig. 3.

Notations used in Fig. 3:

$d_{F,\max}$ – maximum Feret's diameter, largest distance between two parallel lines adjacent to the object contour;
$d_{F,h}$ – horizontal Feret's diameter, distance between two parallel lines measured horizontally;
$d_{F,v}$ – vertical Feret's diameter, distance between two parallel lines measured vertically;
$d_{M,h}$ – horizontal Martin's diameter, length of a segment of the inside object contour secant (chord), dividing the object projection area into two equal parts, measured parallel to the horizontal direction;
$d_{M,v}$ – vertical Martin's diameter, length of a segment of the inside object contour secant, dividing the object projection area into two equal parts, measured parallel to the vertical direction;
a_1 – length of the major axis of an ellipse bounding an object;

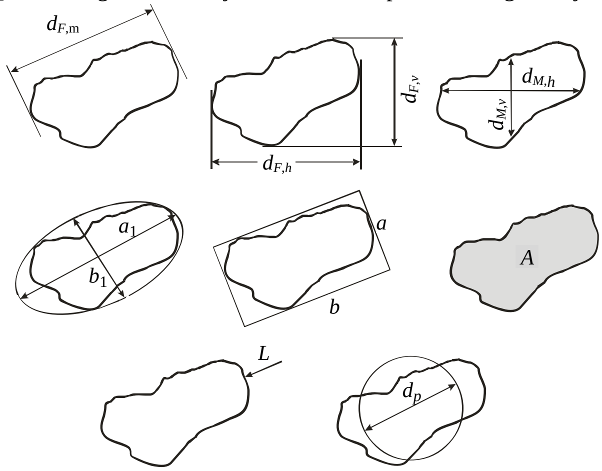

Fig. 3. Geometric parameters of an object (pore) [7]

b_1 – length of the minor axis of an ellipse bounding an object;
a – height of a rectangle bounding an object;
b – width of a rectangle bounding an object;
A – surface area of object projection;
L – object circumference;
d_p – projection diameter.

The size of pores can only indirectly affect porosity. This particularly refers to the pore shapes: as a bubble increases, the force of displacement also increases while the bubble is floating up towards the liquid surface, and simultaneously, the gas pressure inside the pore decreases. These changes lead to larger bubble deformation (Figs 2, 4).

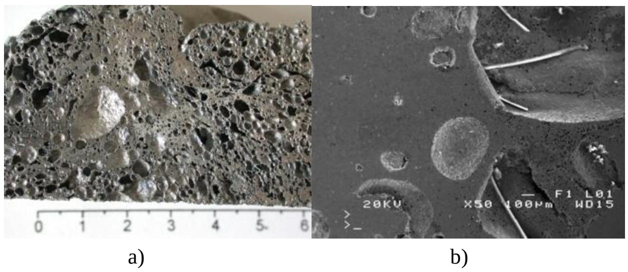

a) b)

Fig. 4. Various shapes and sizes of pores in metal composite foams: a) macroscopic examination, b) SEM

The size of a single bubble may be determined by the image analysis method, and the mean magnitude, in turn, can only be calculated as an arithmetic mean or by means of more advance statistical methods (Tab. 1–3). The tables and figures below present the results, through the use of stereology and statistics for the description of composite foam structure properties, of comparison of pore size and shape, based on 10 selected analysis fields. Kruskal-Wallis tests results are presented for the surface area and shape coefficient of the pores, in which case first the distribution was checked for being normal or not. The Kolmogorov test results are given in Tables 1 and 2. As in most cases there is a deviation from the normal distribution, in each analyzed field ($p < 0.05$) a Kruskal-Wallis test was applied for a comparison of examined fields (Figs 5–6).

Table 1.
Quantitative description of a planar cross-section shape of composite foam pores

Analysis field	**Mean [mm]**	SD [mm]	Coeff. of variation [%]	Min [mm]	Quartile_1 [mm]	Median [mm]	Quartile_3 [mm]	Max	**Kolmogorov test result**
1	**0.630**	0.159	25.2%	0.220	0.535	0.640	0.740	1.000	**> 0.05**
2	**0.585**	0.160	27.3%	0.190	0.488	0.615	0.693	1.000	**> 0.05**
3	**0.601**	0.178	29.5%	0.180	0.490	0.620	0.720	1.000	**> 0.05**
4	**0.615**	0.143	23.3%	0.240	0.540	0.630	0.720	1.000	**> 0.05**
5	**0.625**	0.158	25.2%	0.240	0.523	0.630	0.720	1.000	**> 0.05**
6	**0.609**	0.164	26.9%	0.220	0.490	0.620	0.715	1.000	**> 0.05**
7	**0.648**	0.149	23.0%	0.180	0.560	0.630	0.750	1.000	**> 0.05**
8	**0.636**	0.164	25.7%	0.150	0.540	0.650	0.740	1.000	**> 0.05**
9	**0.632**	0.149	23.5%	0.240	0.530	0.640	0.730	1.000	**> 0.05**
10	**0.638**	0.182	28.6%	0.170	0.520	0.645	0.750	1.000	**> 0.05**

Table 2.
Quantitative description of a planar cross-section shape of composite foam pores

Analysis field	**Mean [mm²]**	SD [mm²]	Coeff. of variation [%]	Min [mm²]	Quartile_1 [mm²]	Median [mm²]	Quartile_3 [mm²]	Max [mm²]	**Kolmogorov test result**
1	**75.30**	83.12	110.4%	1.15	16.69	45.42	103.38	426.92	**< 0.01**
2	**65.72**	69.59	105.9%	1.32	20.49	47.98	85.98	480.85	**< 0.01**
3	**81.31**	81.45	100.2%	1.05	24.03	64.20	111.14	488.04	**< 0.01**
4	**85.25**	85.22	100.0%	1.55	21.61	58.02	114.97	441.99	**< 0.05**
5	**72.93**	74.28	101.9%	1.01	24.58	45.50	96.66	318.62	**< 0.01**
6	**76.39**	76.03	99.5%	1.08	18.31	51.90	108.72	404.41	**< 0.02**
7	**71.63**	77.01	107.5%	1.35	19.53	43.32	101.04	429.92	**< 0.01**
8	**78.71**	82.18	104.4%	1.05	19.46	42.68	106.04	405.43	**< 0.01**
9	**76.72**	70.21	91.5%	1.01	24.63	57.14	105.61	304.22	**< 0.05**
10	**59.13**	75.47	127.6%	1.15	10.36	37.90	77.26	514.81	**< 0.01**

Table 3.
Quantitative description of the maximum diameter, minimum diameter, Feret X diameter, Feret Y diameter of a planar cross-section of composite foam pores

Analysis field	Mean [mm]	SD [mm]	Coeff. of variation [%]	Mean [mm]	SD [mm]	Coeff. of variation [%]	Mean [mm]	SD [mm]	Coeff. of variation [%]	Mean [mm]	SD [mm]	Coeff. of variation [%]
	maximum diameter			**minimum diameter**			**Feret X diameter**			**Feret Y diameter**		
1	**12.95**	7.21	55.7%	**7.16**	4.41	61.6%	**10.00**	5.51	55.0%	**10.78**	6.85	63.5%
2	**12.86**	6.57	51.0%	**6.63**	3.93	59.2%	**10.31**	5.96	57.8%	**10.02**	5.60	55.9%
3	**13.71**	6.90	50.3%	**7.75**	4.55	58.7%	**10.86**	6.24	57.5%	**11.25**	6.04	53.7%
4	**14.14**	7.28	51.5%	**7.84**	4.25	54.1%	**11.35**	6.36	56.1%	**11.39**	6.03	52.9%
5	**13.46**	7.14	53.1%	**6.95**	4.07	58.5%	**10.32**	6.26	60.7%	**10.72**	6.10	56.9%
6	**13.40**	7.21	53.8%	**7.14**	4.14	58.0%	**10.69**	6.41	60.0%	**10.67**	5.94	55.6%
7	**12.65**	6.86	54.3%	**6.94**	4.09	58.9%	**10.25**	5.93	57.9%	**9.89**	5.86	59.3%
8	**13.24**	7.53	56.8%	**7.39**	4.56	61.7%	**10.31**	6.24	60.5%	**11.04**	6.79	61.4%
9	**13.52**	7.02	51.9%	**7.48**	3.99	53.4%	**10.53**	5.75	54.5%	**11.26**	6.05	53.7%
10	**11.47**	6.95	60.6%	**6.15**	4.27	69.3%	**9.27**	6.53	70.4%	**8.96**	5.52	61.6%

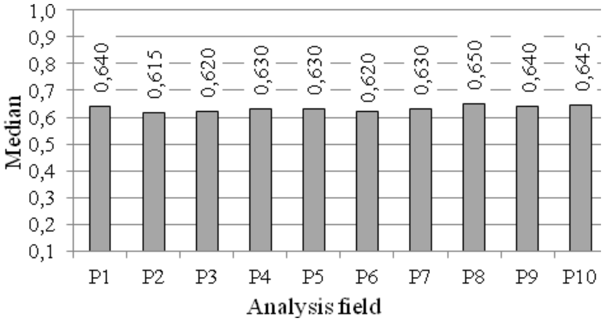

Fig. 5. Values of the median of a dimensionless shape coefficient for a planar cross-section of composite foam pores

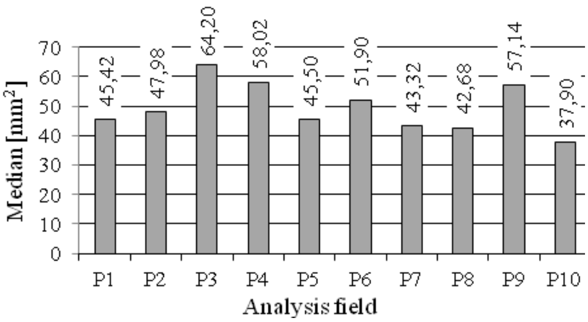

Fig. 6. Values of the surface area median of planar cross-sections of composite foam pores, results of a Kruskal-Wallis test

The ratio of actual to maximum porosity

The ratio of actual porosity to maximum can be assumed as a parameter well characterizing foam structure. There may be a 'film' of metal between two bubbles of certain thickness, below which those bubble will join. Using the image analysis method we can determine a total area of boundaries between bubbles. The minimum thickness of the 'film' may be assumed to be the least thickness directly measured in a sample cross-section. The maximum porosity can be determined from this relationship:

$$P_{\max} = 1 - \frac{g \cdot s}{V_c} \quad (2)$$

where:

- g – minimum thickness of metal film,
- s – area of bubble boundaries in a sample,
- V_c – sample volume.

Then the ratio of actual porosity to maximum porosity will take this value:

$$S = \frac{P_{rz}}{P_{\max}} \quad (3)$$

where: P_{rz} – actual porosity of a sample.

Homogeneity of foam structure

The considered foam homogeneity can refer to three different features of pores: size, distribution, shape.

For practical reasons instead of homogeneity, we will illustrate corresponding types of inhomogeneity. The three types are illustrated in Fig. 7.

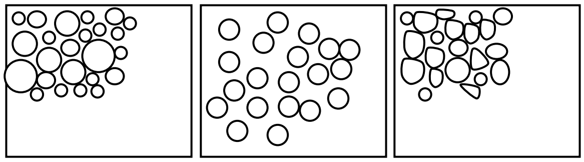

a) b) c)

Fig. 7. Example types of porosity inhomogeneity: a) inhomogeneity of size, b) inhomogeneity of distribution, c) inhomogeneity of shape

The size of pores that do not have regular shapes may be determined by measuring their cross-section area. Size inhomogeneity is best characterized by a distribution curve, depicted in Fig. 8.

For practical reasons the value of mean standard deviation of the results or the value 3σ can be utilized [8]. Pore distribution inhomogeneity can be determined by measuring the mean size of pores in various places of foam sample cross-section.

3. Conclusions

The above considerations constitute a proposition of the description of geometric structure of metal composite foams. A systematic description of those materials will contribute to their qualitative evaluation, also at the stage of manufacturing. Besides, consistent description of geometric properties of metal foams may contribute to better communication between researchers and manufacturers of these interesting materials.

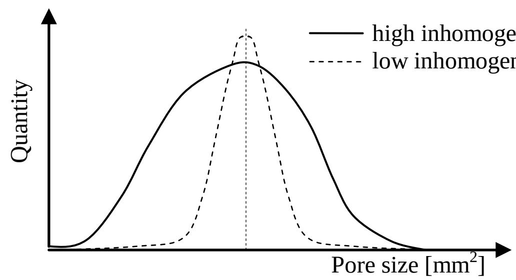

Fig. 8. Distribution of pore sizes within a sample cross-section

References

[1] Gawdzińska, K., Grabian, J., Pędzich, Z. & Przetakiewicz, W. (2011). A Description of Particle Shape Homogeneity in the Space of Composite Suspension Casting. *Archives of Foundry Engineering*. 11(spec. 1), 11-14.

[2] Gawdzińska, K. & Wojnar, Z. (2008). Application of microtomograhpy in the detection and quantification of defects cast composites. *Archives of Foundry Engineering*. 8(1), 103-108.

[3] Grabian, J. & Przetakiewicz, W. (2009). Assessment of possible control of selected operational properties of metal-ceramic forms. *Archives of Foundry Engineering*. 9(4), 419-422.
[4] Szweycer, M. (1996). *Surface phenomena in foundry*. Kraków: Wydawnictwo Instytutu Odlewnictwa.
[5] Grabian, J. (2012). *Composite metal foam in the shipbuilding*. Kraków: Wydawnictwo Fotobit.
[6] Kraynik, A.M., Douglas, A.R. (2012). Foam Microrheology: from honeycombs to random foams. Retrieved, from www.scribit.com.
[7] Krawczyńska, A. (2007). *Recognition in the identification of ore types and their properties in products processing of copper ore*. Unpublished doctoral dissertation, AGH, Kraków.
[8] Gawdzińska, K. (2012). Material and technological conditions of quality of metal composite castings. Katowice-Gliwice: *Archives of Foundry Engineering*.

Charakterystyczne cechy struktury geometrycznej pian metalowych

Opis materiału powinien odbywać się na zasadzie opisu jego cech charakterystycznych. Niestety w przypadku metalowych pian kompozytowych opisu takiego nie stwierdzono. Postanowiono zatem przedstawić propozycję opisu struktury geometrycznej tych tworzyw dzieląc te cechy na: porowatość, kształt i wielkość porów, stosunek porowatości rzeczywistej do maksymalnej, powierzchnię właściwa pęcherzy oraz jednorodność budowy piany, gdzie wyodrębniono jednorodność wielkości, kształtu i rozmieszczenia porów. Praca ta ma charakter otwarty i jest propozycją opisu struktury geometrycznej pian metalowych.